Scanning Electron Microscopy

Volume 1985
Number 1 *1985*

Article 3

10-8-1984

Some Considerations of the Ultimate Spatial Resolution Achievable in Scanning Transmission Electron Microscopy

Anthony J. Garratt-Reed
Massachusetts Institute of Technology

Follow this and additional works at: https://digitalcommons.usu.edu/electron

Part of the Biology Commons

Recommended Citation

Garratt-Reed, Anthony J. (1984) "Some Considerations of the Ultimate Spatial Resolution Achievable in Scanning Transmission Electron Microscopy," *Scanning Electron Microscopy*: Vol. 1985 : No. 1 , Article 3.
Available at: https://digitalcommons.usu.edu/electron/vol1985/iss1/3

This Article is brought to you for free and open access by the Western Dairy Center at DigitalCommons@USU. It has been accepted for inclusion in Scanning Electron Microscopy by an authorized administrator of DigitalCommons@USU. For more information, please contact digitalcommons@usu.edu.

SCANNING ELECTRON MICROSCOPY/1985/I (Pages 21-29)
SEM Inc., AMF O'Hare (Chicago), IL 60666 USA

0586-5581/85$1.00+.05

SOME CONSIDERATIONS OF THE ULTIMATE SPATIAL RESOLUTION ACHIEVABLE IN SCANNING TRANSMISSION ELECTRON MICROSCOPY

Anthony J. Garratt-Reed

Center for Materials Science and Engineering
Massachusetts Institute of Technology
Cambridge, Massachusetts 02139

(Paper received March 14 1984, Completed manuscript received October 8 1984)

Abstract

The fundamental limitations on spatial resolution of X-ray microanalysis in the scanning transmission electron microscope are set by the interrelationships between the gun brightness, operating voltage, probe convergence angle, size and current, specimen thickness, beam broadening, the probability of characteristic and Bremsstrahlung X-ray production and the statistics of the X-ray spectrum. Manipulation of expressions describing these interrelationships leads to equations predicting the optimum probe size and specimen thickness for the best achievable spatial resolution (defined as the diameter of a cylinder containing 90% of the X-ray production) in microscopes fitted with different electron sources and operating at different voltages in foils of various elements. Application of these calculations to the special case of detecting monolayer segregation at grain boundaries results in predictions of the minimum amounts of such segregation that would be observable. It is found, for example, that in a microscope with a field-emission source operating at 500 keV, resolution of < 1nm is obtainable in an iron foil 20nm thick, and in this case about 0.001 monolayer of chromium is detectable segregated at grain boundaries. The calculations do not take into account instrumental or experimental problems such as specimen drift, specimen preparation, etc., and represent the basic physical limits of performance of a perfect analytical microscope.

KEY WORDS: Spatial Resolution, Analytical Electron Microscopy, X-ray Microanalysis, High Voltage Microscopy.

Address for correspondence:
M.I.T., Room 13-1027
Cambridge, MA. 02139
U.S.A.
Phone No.: (617) 253-4622

Introduction

The analysis of fine-scale elemental segregation in thin foils using a scanning transmission electron microscope (STEM) equipped with an energy dispersive X-ray detector is limited by the problem of beam broadening, and indeed that of the inherent relationship between probe current and beam diameter. It is obvious, for example, that in an infinitely thin sample the spatial resolution is determined by the probe size; equally obviously, in such a case the X-ray signal is infinitely small, and the elemental sensitivity becomes vanishingly low. While much thought has been given to these problems, authors have tended not to consider the possibility of working with foils less than about 100nm thick (e.g. Goldstein et al, 1977, Doig et al, 1980). In this paper we shall discuss fine-scale microanalysis in STEM, without regard to the experimental difficulties involved. We shall consider the use of thermionic tungsten or field emission electron sources, and consider the possibility of operation at electron energies up to 500 keV. By so doing, it becomes possible to identify the practical limits on spatial resolution, and to direct efforts in appropriate directions to improve these limits.

Statistics

It is necessary first to consider briefly the statistics of the energy dispersive X-ray spectrum. There are two quite distinct problems to address. The first is the precision of an analysis when all elements are present at levels significantly above their detectability limits, which has been considered elsewhere (e.g. Ziebold, 1967, Goldstein et al, 1981) and will not be pursued here. We will note, however, that it is always possible to specify (perhaps after a pilot run has been made) the minimum number of counts that must be acquired in order to achieve the desired precision in the result.

The second problem concerns the minimum detectable concentration of an element X in a matrix M (which may contain more than one element). The spectrum recorded in an energy-dispersive X-ray analysis system consists of a series of characteristic X-ray lines superimposed upon a continuum

Table of Symbols

A	atomic weight
B	gun brightness
b	beam broadening in sample
b_{90}	diameter of cylinder enclosing 90% of X-ray production
b_k, c_k	fitting parameters
C_s	spherical aberration of probe-forming lens
d	diameter of electron probe
E_k	ionization energy of K-shell electron
e	charge on electron
i_p	electron probe current
m_o	electron rest-mass
N	X-ray count-rate
N_{bk}	number of X-ray counts in background in region of interest
N_m	number of X-ray counts from matrix elements
N_o	Avogadro's number
N_X	number of X-ray counts from element X
N_{Xmin}	minimum detectable number of X-ray counts from element X
s	fraction of total K-radiation emitted in K_α line
t	specimen thickness
V	electron energy
v	electron velocity
ε	detector efficiency
σ_k	K-shell ionization cross-section
ρ	specimen density
ω_k	fluorescence yield for K X-ray emission

Bremsstrahlung background. The problem, then, is to determine when the peak corresponding to element X can be detected above the background.

Goldstein et al (1981) have reviewed several methods to achieve this end. More recently, Chapman et al (1983) have shown that in the absence of instrumental artefacts, a modified Bethe-Heitler formula may be used to predict accurately the background shape to within 2% over the energy range 3-20 keV. If the predicted background is then normalized to the acquired spectrum near the region of interest, the precision of the fit will be determined essentially by the statistics of the fitting regions. In the case of a simple spectrum a large number of channels may be used for fitting the background, so that the uncertainty in the prediction of the background within the region of the characteristic peak of X can be made small compared with the statistical uncertainty of the total number of counts in the region. It has been shown that in these circumstances the minimum significant deviation from the background is given by:

$$N_{Xmin} = 2\sqrt{N_{bk}} \qquad (1)$$

where N_{Xmin} is the minimum number of counts which can, with 97.5% certainty be said to indicate the presence of element X in the sample (Joy and Maher, 1977). This minimum number of counts can be related to a "minimum detectable composition" by relating N_{Xmin} to N_m by the conventional methods of quantitative thin film microanalysis (e.g. the "K-factor" method of Cliff and Lorimer, 1975). Again it is possible to specify the minimum number of counts that must be acquired in order to reach any desired sensitivity in an experiment.

Once the minimum number of counts required has been specified, it becomes possible to define a required count-rate, the time available for counting being limited by factors such as radiation effects in the sample (mass loss, etc), specimen drift, contamination, and the operator's productivity. Generally an upper time limit of 100 seconds is reasonable, and this time will be assumed in the examples quoted in this paper.

There is an upper limit on the achievable count-rate set by the X-ray detector, which is typically 2000 cps. This arises because the analysis of each arriving X-ray takes a finite time during which no other X-ray can be detected (e.g. Fiori and Newbury, 1978). Thus there is a lower limit on the minimum detectable concentration of element X in matrix M.

Characteristic X-ray Emission

In this section we shall review briefly the production of characteristic X-rays.

The number of K_α X-rays generated per second in a thin foil can be obtained from:

$$N_X = \frac{i_p}{e} \cdot \frac{N_o}{A} \rho t \, \sigma_k \, \omega_k \, s \qquad (2)$$

Similar equations may be written for X-ray lines of other series. Of these factors, ω_k and s may be obtained, ω_k for example from Langenberg and van Eck (1979), and s from Schreiber and Wims (1982)

The cross section, σ_k is less well-known. Powell (1976) presented a thorough review of the data available at that time, from the point of view of the microprobe user interested in electron energies well below 100 keV, where relativistic effects are negligible. Cross-sections based on Powell's paper have been widely applied with success at electron energies up to 100 keV. At this voltage, however, the difference between the electron kinetic energy and 0.5 $m_o v^2$ already exceeds 20%, and it is not to be expected (nor did earlier authors represent) that these non-relativistic methods would be appropriate for use with higher energy electrons.

Rez (1984) has performed exact numerical calculations to predict σ_k for a number of elements. These calculations, while accurate, require substantial computer time, and for routine use, a simpler method of finding the cross-section is preferred. Chapman et al (1984) have measured cross-sections for a range of elements at electron energies from 40 keV to 100 keV, and fitted them to a relativistic form of the Bethe equation (e.g. Mott and Massey, 1965) in which the cross-section is given by:

$$\sigma_k = \frac{4\pi e^4}{m_o v^2 E_k} \cdot b_k \, \ell n \left(\frac{c_k m_o v^2}{2E_k}\right) \qquad (3)$$

They found that the best fit to their data was obtained when $b_k = 0.58$ and $c_k = 0.99$.

Zaluzec (1984) used a very similar equation, but allowed b_k and c_k themselves to vary with atomic number. By fitting to selected data from the literature at electron energies up to 1 MeV he has derived polynomial equations in atomic number from which b_k and c_k may be obtained. For the case of ionization of iron the cross-sections given by these two equations agree to within 1% for 100 keV electrons, and differ by about 15% for 500 keV electrons. For the purposes of the estimates to be made in this paper, either cross-section would probably be adequate (as will be seen, the cross-section will be taken to the power 0.3 in the expressions to be derived). We shall for convenience use the simpler representation of Chapman et al (1984).

X-ray Generation and Detection in Thin Foils

In a thin elemental foil the number of characteristic X-rays produced per second is given by equation 2. The number N detected per second may be obtained from:

$$N = P\rho t i_p \sigma_k \varepsilon \qquad (4)$$

where the parameter P is given by

$$P = \frac{N_o}{e} \cdot \frac{1}{A} \cdot \omega_k s \qquad (5)$$

where the value of each quantity appropriate for the element of the foil is used.

The efficiency of the detector is governed by two independent effects. The first, which determines the relative sensitivity of the detector to X-rays of different energies, is the physics of its operation. This has been discussed in the literature by, for example, Fiori and Newbury (1978), and we merely note here that for the K lines of medium atomic weight elements such as chromium and iron the relative detector efficiencies are sufficiently similar that we may take them to be equal, and for our purposes we may assume that every X-ray that enters the detector is detected. The second effect is the solid angle subtended at the specimen by the detector crystal. For example, a detector with $30mm^2$ active area 19mm from the sample (about the largest that may be fitted into the Vacuum Generators HB5) will have an efficiency of 0.006, and we shall use this value in the following calculations.

We may now substitute numerical values in equation 4 and obtain, for the example of an iron foil:

$$N = 0.0945\ t\ i_p\ \sigma_k \qquad (6)$$

if i_p is measured in nanoamps, t in nanometers and σ_k in barns. Since from the statistical analysis, the required count rate N is known, we may rewrite equation 6 as follows:

$$t \cdot i_p = \frac{N}{0.0945\ \sigma_k} \qquad (7)$$

In other words, to achieve the desired count rate, the product $t \cdot i_p$ must have the appropriate value.

Spatial Resolution

It has been the practice to define the spatial resolution for X-ray microanalysis as being the diameter of a cylinder which encloses the volume in which 90% of the X-rays are produced. Imeson (1982) has pointed out that this definition is useful if the composition varies slowly over the dimensions of the cylinder. Let us now consider how small this volume can be made. For our example we shall consider the detection of small amounts of chromium in iron.

Beam Broadening

As electrons travel through the sample, they undergo elastic and inelastic interactions which result in the beam spreading. The situation is illustrated in Fig. 1. If an elemental composition profile in a sample is measured in such conditions, the measured profile will represent a convolution of the actual profile, the incident probe size and the beam broadening, integrated over the specimen thickness.

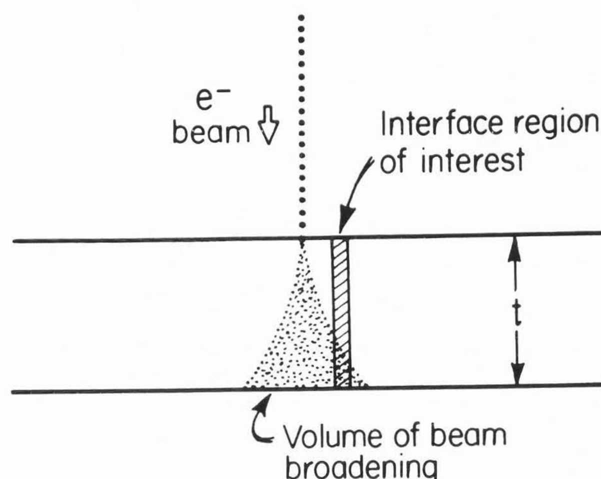

Fig. 1. Schematic illustration of the interaction of an electron probe with a foil containing segregation in a narrow planar region.

In order to make quantitative measurements, therefore, it is necessary to know the extent of the beam broadening. There have been a number of attempts to predict and measure beam broadening, the predictions being based upon Monte Carlo calculations (e.g. Kyser, 1979), the "single scattering" model of Goldstein et al (1977) or the transport equation (Imeson, 1982), and the measurements being made by determining the X-ray signals obtained from the gold bars deposited on either the upper or lower surface of a sample (Hutchings et al, 1979, Stephenson et al, 1981).

Fries et al (1982) have also compared measured profiles with those predicted by the single scattering model.

It is not the intent of this paper to review these methods. We note the following:

(i) All models apply strictly only to amorphous specimens. They are probably also reasonably good for an electron beam travelling in some random high-order direction in a crystal, but they are definitely not applicable to cases when the electron beam is parallel to a zone axis, or if significant diffraction is occurring. It was suggested by Imeson and Vander Sande (1981) and has been demonstrated theoretically by Marks (private communication) that if the specimen is crystalline and the electron beam is oriented parallel to a low-order axis then diffraction theory predicts that the beam will suffer reduced inelastic scattering. The beam broadening in such cases is more nearly dependent upon the thickness rather than $t^{3/2}$ (see below). He has also predicted, and Vander Sande et al (1984) have shown in practice that if significant diffraction is occurring, then the effective shape of the beam broadening profile will be changed, changing the predictions of effective spatial resolution and grain boundary detectability that are derived in this paper.

(ii) Within the limits of the foregoing caveat, the beam broadening b appears to obey a law of the form:

$$b = \frac{k}{V} \cdot f(Z,A,\rho)t^{3/2} \qquad (8)$$

where k is a constant and $f(Z,A,\rho)$ indicates that the broadening depends upon the atomic number, atomic weight and density of the sample.

There are some indications (Kerr et al, 1981, Fries et al, 1982) that the single scattering model of Goldstein et al (1977) overestimates the beam broadening. We will therefore use the data of Kerr et al (1981) who computed the diameter within which 90% of the X-rays are produced in various thicknesses of copper. This data will slightly overestimate the broadening in iron, but for our purposes will be adequate. The data of Kerr et al (1981) may be represented by the equation:

$$b_{90} = \frac{1760\ t^{3/2}}{V} \qquad (9)$$

where b_{90} and t are measured in nanometers.

Probe Diameter.

The current in the electron probe is given by:

$$i_p = \frac{\pi^2 (d)^{8/3}}{4(C_s)^{2/3}} \cdot B \qquad (10)$$

For a typical modern lens, C_s is 3mm; we shall take the brightness of a field-emission electron source to be 5×10^3.V A/cm^2/Sr, and a tungsten gun to be 5.V A/cm^2/Sr. Thus equation 9 becomes:

$$i_p = 5.9\text{x}10^{-6} V\ d^{8/3} \text{ for a field emission gun} \qquad (11a)$$

$$i_p = 5.9\text{x}10^{-9} V\ d^{8/3} \text{ for a tungsten gun} \qquad (11b)$$

where d is now measured in nanometers and i_p in nanoamps.

Optimum Resolution

To achieve optimum spatial resolution, clearly the optimum choice of probe diameter (and hence probe current) and beam broadening (and therefore specimen thickness) must be made. The exact optimum relationship between d and b is not clear, but it is obvious that if one is much larger than the other, the spatial resolution will be determined solely by the larger one, and could be improved by altering the experimental conditions. For our purposes we shall assume that the optimum occurs when b and d are equal, when the spatial resolution will be determined equally by these two parameters.

Equation 9 may therefore be rewritten:

$$t = \left(\frac{dV}{1760}\right)^{2/3} \qquad (12)$$

and we may then substitute in equation 7 and rearrange to obtain:

$$d = \left(\frac{2.615 \times 10^8\ N}{V^{5/3}\ \sigma_k}\right)^{0.3} \qquad (13a)$$

for the field-emission case, and:

$$d = \left(\frac{2.615 \times 10^{11}\ N}{V^{5/3}\ \sigma_k}\right)^{0.3} \qquad (13b)$$

for the tungsten case. These equations can then be solved to obtain d, the probe diameter for optimum spatial resolution. Once d has been found, substitution in equation 12 gives the optimum value of specimen thickness t. Values of d and t have been computed for electron energies between 100 keV and 500 keV, for count rates of 50cps and 2000cps in the characteristic peak, and for field-emission and tungsten electron sources. The results are presented in Table 1. It must be remembered that the figures for d do not represent spatial resolution directly -- that figure is obtained from a convolution of b and d, and is probably closer to 2d. It should also be noted that the value given for d for the case of low count rates in the field-emission case may be at or below the diffraction limit of the probe forming lens, and if so, would not be achievable in practice.

Fig. 2 is an example of high spatial resolution microanalysis which is consistent with the above calculations (from Garratt-Reed et al 1984). The specimen was a chromium pearlite, and a chromium analysis was obtained across a cementite plate, using a field-emission microscope operating at 100 kV, the foil being about 20nm thick. The X-ray count rate was about 60cps in the iron peak, and the detector efficiency was 1.2×10^{-3}. Independent atom probe studies on this material (Williams et al, 1983) have shown that just inside the cementite is a region about 2nm wide enriched in chromium to levels $\sim$ 6%, dropping to $\sim$ 3% in the center of the cementite. These features can be seen to be accurately reproduced in the STEM result.

TABLE 1

Predictions of values of optimum beam diameter d and specimen thickness t (both in nanometers) for best spatial resolution in iron foils studied in field-emission and tungsten microscopes at various operating voltages, and for 2000cps and 50cps in the characteristic iron peak.

	FE				W			
kV	50 cps		2000 cps		50 cps		2000 cps	
	d	t	d	t	d	t	d	t
100	0.60	10.5	1.81	21.9	4.76	41.8	14.4	87.5
200	0.46	14.0	1.40	29.4	3.68	55.9	11.1	116.7
300	0.40	16.7	1.19	34.5	3.14	65.9	9.5	137.8
400	0.35	18.5	1.06	38.7	2.79	73.8	8.4	154.1
500	0.32	20.2	0.96	42.1	2.53	80.2	7.7	168.1

Segregation at Grain Boundaries

It is quite easy to compute the X-ray signal that would be measured when an electron probe is placed at some point in a concentration distribution in a foil of known thickness if one assumes a model for beam broadening (Doig et al, 1980, Hall et al, 1981). The reverse process, deconvolving a measured profile to obtain the actual profile, is mathematically quite straightforward; unfortunately, the deconvolution is very intolerant of errors in the measurements, so in most cases it becomes impractical because of the statistical scatter of the data. If, however, the shape of the actual profile is known or can be approximated well, as, for example, when monolayer segregation at a grain boundary is being studied, the problem is simplified. Combining the data of Table 1, computations of the type of Doig et al (1980) or Hall et al (1981) and estimates of minimum detectable concentration, it is possible to estimate the minimum fraction of a monolayer that would be detectable under ideal conditions. The experiment under consideration consists of locating a grain boundary parallel to the electron beam, obtaining an X-ray spectrum with the probe located on the boundary, and finding a criterion for the minimum fraction of a monolayer that must be present to give a detectable signal in the X-ray spectrum.

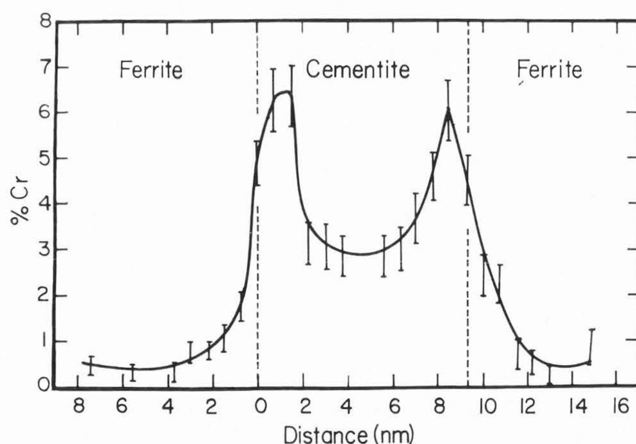

Fig. 2. Plot of apparent chromium composition as a function of position across a cementite plate in a chromium pearlite. Spatial resolution of the order of 2 nm is demonstrated.

Peak to Background Ratios

The minimum detectable concentration of a trace element is clearly dependent upon the peak to background ratios of the elements in the sample. In this discussion, the term 'peak to background ratio' means the number of counts in a given window in the spectrum due to characteristic emission from an element of interest divided by the number of counts in the same window due to Bremsstrahlung radiation, and is therefore a function of the window width chosen and of the energy resolution of the detector and the energy of the X-ray line as well as the physics of generation and detection of the spectrum.

Bremsstrahlung emission from a sample under electron bombardment has been considered by Zaluzec (1978) and by Chapman et al (1983). The Bremsstrahlung X-rays are not emitted isotropically, but predominantly in a 'forward' direction, where forward means in the direction in which the electrons are travelling. Chapman et al (1983) studied experimental spectra obtained from various elements using electrons in the range 40 - 100 keV, and found that the cross-section for Bremsstrahlung emission can be well represented by a modified Bethe-Heitler formula. There are constraints in the formulation that restrict its application to photon energies below some maximum, and to electron energies above some minimum, but Chapman et al (1983) show for the range of photon and electron energies under

consideration in this paper their results should be applicable.

Combining the results of Chapman et al (1983) and Chapman et al (1984) it is therefore possible to predict the peak to background ratio for any element, electron energy and microscope geometry. Table 2 presents such a prediction for iron, for the geometry of the VG HB5, in which the detector is at an angle of 100.5° to the incident beam, and for electron energies up to 500 keV.

TABLE 2

Estimated peak/background ratio for iron at variour voltages. The X-ray detector was assumed to be at 100.5° to the electron beam. A window 200 eV wide centered on the iron K energy was assumed.

Electron energy (keV)	Peak/background
100	184
200	268
300	349
400	432
500	516

Once the peak to background ratio is known, it becomes possible, using the calculations described in the section on statistics, to determine the minimum detectable composition. Table 3 shows the results of such a computation, for detecting chromium in iron. The program of Hall et al (1981) was used to predict the X-ray signal that would be observed when electron probes of various sizes are incident upon grain boundaries in various thicknesses of foils. Doig and Flewitt (1983) have shown that provided the maximum detector count rate is not exceeded, then for a given foil thickness the detectability of grain boundary segregation is maximized by maximizing the electron current. Therefore, the beam diameters and foil thicknesses appropriate for best resolution of 2000 cps were used in the computations. The grain boundary was modelled by a Gaussian distribution of chromium of full-width at half-maximum of 0.2 nm. The broadening was set to 0.7 times that predicted by Goldstein et al (1977). The program outputs the apparent concentration that would be measured in the X-ray spectrum, which may be related to the minimum detectable concentration (Table 3) to deduce the minimum fraction of a monolayer that would be detectable. Table 4 gives the results.

Doig and Flewitt (1982) deduced from empirical results in a microscope with a tungsten source operating at 100 kV that approximately 0.2 monolayer of phosphorous and 0.01 monolayer of tin are detectable on a grain boundary in steel. While this data is not directly comparable with the present work, nevertheless the equivalent prediction that 0.04 monolayer of chromium would be detectable in such an experiment is in reasonable agreement with their work. However, this work predicts a marked increase in the detectability of grain boundary segregation as the electron energy is increased, in contrast to the result of Doig and Flewitt (1982). This difference arises mainly because they did not take into account the increase in gun brightness with accelerating voltage and the increase in peak-to-background ratio with increasing electron energy, and also because they used a non-relativistic prediction of the variation of X-ray production with operating voltage.

TABLE 3

Prediction of minimum detectable concentration of chromium in iron at electron energies up to 500 keV.

Electron energy	Minimum detectable conc.
(keV)	(wt. %)
100	0.04
200	0.032
300	0.027
400	0.024
500	0.021

TABLE 4

Estimated minimum fraction of a monolayer of chromium detectable on a grain boundary in iron at various voltages in field-emission and tungsten microscopes.

Electron energy (keV)	Fe	W
100	0.005	0.04
200	0.003	0.024
300	0.002	0.017
400	0.0017	0.014
500	0.0014	0.011

Experimental Considerations

In this paper no consideration has been given to experimental problems. In fact, of course, usually the limits of spatial resolution are determined by such factors as specimen drift, contamination, or inability to control the microscope with sufficient precision. It is also necessary to ascertain that the thin foils required for high spatial-resolution analysis are representative of the bulk.

It has been tacitly assumed throughout this paper that the electron probe has a Gaussian shape; however, amongst others, Kenway and Cliff (1984) have shown that in many cases the probe may depart significantly from a Gaussian form. Indeed, there is evidence of such departure in Fig. 2, where the skirts of the chromium concentration up to $\sim$ 4nm either side of the cementite, which do not appear on computer models, are quite possibly due to non-Gaussian skirts around the electron probe. A complete treatment of spatial resolution should include provision for this effect, the mathematical

formulation having been provided by Kenway and Cliff (1984).

Summary

It has been shown that by using a field-emission gun in a STEM operated at 500 kV, it could be physically possible to achieve spatial resolution for X-ray microanalysis of thin foils of < 1nm in suitable samples provided the drift rate and sample contamination can be minimized. It should also be possible to detect grain boundary segregation as little as 0.0015 monolayer of chromium in iron if the electron probe can be positioned with sufficient accuracy on the boundary. As the limits of microanalysis in both cases are related to the microscope, there appears to be considerable incentive to improve further the stability of instruments with field-emission guns, and to operate analytical electron microscopes at as high an electron energy as is possible.

Acknowledgements

This work was funded by the National Science Foundation under Block Grant number DMR 81-19295. The author also wishes to thank Dr. W.A.P. Nicholson for reading the final manuscript and for helpful discussions.

References

Chapman JN, Gray CC, Robertson BW, Nicholson WAP (1983) "X-ray production in thin films by electrons with energies between 40 and 100 keV", X-ray Spectrom. 12, 153-156.

Chapman JN, Nicholson WAP, Crozier PA (1985) "Understanding thin film X-ray spectra", presented at conference on electron-specimen interactions, Cambridge, 1983, J. Microsc., in press.

Cliff G, Lorimer GW (1975) "The quantitative analysis of thin specimens", J. Microsc. 103, 203-207.

Doig P, Lonsdale D, Flewitt PEJ (1980) "The spatial resolution of X-ray microanalysis in the scanning transmission electron microscope", Phil. Mag. A41, 761-775.

Doig P. Flewitt PEJ (1982) "The detection of monolayer grain boundary segregation in steels using STEM-EDS X-ray microanalysis", Met. Trans. A 13A, 1397-1403.

Doig P, Flewitt PEJ (1983) "The role of specimen and instrumental parameters in STEM-EDS X-ray microanalysis in thin foils", J. Microsc. 130, 377-388.

Fiori C, Newbury DE (1978) "Artifacts observed in energy-dispersive X-ray spectrometry in scanning electron microscopy", Scanning Electron Microsc. 1978; I:401-422.

Fries E, Imeson D, Garratt-Reed AJ, Vander Sande JB (1982) "Spatial resolution for compositional analysis in STEM", Ultramicroscopy 9, 295-302.

Garratt-Reed AJ, Mottishaw TD, Worrall GM, Smith GDW (1984) "First observations of solute redistribution at the pearlite growth front in alloy steels", in "Electron Microscopy and Analysis 1983", Institute of Physics (London) Conference Series number 68, 311-314.

Goldstein JI, Costley JL, Lorimer GW, Reed SJB, (1977) "Quantitative X-ray analysis in the electron microscope", Scanning Electron Microsc. 1977; I:315-324.

Goldstein JI, Newbury DE, Echlin P, Joy DC, Fiori C, Lifshin E (1981) "Scanning Electron Microscopy and X-ray Microanalysis", Plenum Press, New York, ch. 8.

Hall EL, Imeson D, Vander Sande JB (1981) "On producing high spatial-resolution composition profiles via scanning transmission electron microscopy", Phil. Mag A43, 1569-1585.

Hutchings R, Loretto MH, Jones IP, Smallman RE (1979) "Spatial resolution in X-ray microanalysis in thin foils in STEM", Ultramicroscopy 3, 401-411.

Imeson D (1982) "On the spatial resolution of EDX composition determination", Ultramicroscopy 9, 307-310.

Imeson D, Vander Sande JB (1981) "Considerations of the transmission of a small electron probe through a TEM foil and its relation to characteristic X-ray spatial resolution", Proc. 39th. ann. EMSA meeting, ed. GW Bailey, Claitors Publishing Div., Baton Rouge, LA, 282-283.

Joy DC, Maher DM (1977) "Sensitivity limits for thin specimen X-ray analysis", Scanning Electron Microsc. 1977; I:325-334.

Kenway PB, Cliff G (1984) "Electron density distributions in spherically aberrated probes", in "Electron Microscopy and Analysis 1983", Institute of Physics (London) Conference Series number 68, 83-86.

Kerr RT, Titchmarsh JM, Boyes ED (1981) "Simple calculations of X-ray spatial distributions applied to high resolution microanalysis" in "Microbeam Analysis 1981", ed. RH Geiss, San Francisco Press, 333-335.

Kyser DF (1979) "Monte Carlo simulation in electron microscopy", in "Introduction to Analytical Electron Microscopy", eds. JJ Hren, JI Goldstein, DC Joy, Plenum Press, New York, ch. 6.

Langenberg A, van Eck J (1979) "An evaluation of K-shell fluorescence yields; observation of outer shell effects", J. Phys. B 12, 1331-1350.

Mott NF, Massey HSW (1965) "The Theory of atomic collisions", 3rd. edition, Clarendon Press, Oxford, ch. 16.

Powell CJ (1976) "Cross sections for ionization of inner shell electrons by electrons", Rev. Mod. Phys. 48 33-47.

Rez P (1984) "Electron ionization cross-sections for K, L and M shells", X-ray Spectrom. 13, 55-99.

Schreiber TP, Wims AM (1982) "Relative intensity factors for K, L and M shell X-ray lines", X-ray Spectrom. 11, 42-45.

Stephenson TA, Loretto MH, Jones IP (1981) "Beam spreading in thin foils", in "Quantitative Microanalysis with High Spatial Resolution", The Metals Society (London) Book number 277, 53-56.

Vander Sande JB, Garratt-Reed AJ, Chiang Y-M, Thorvaldsson T (1984) "Resolving composition variations at interfaces by STEM", Ultramicroscopy, 14, 65-74.

Williams PR, Miller MK, Smith GDW (1983) "The partitioning of alloy elements during the pearlite transformation: an atom probe study", proceedings of Intl. Conf. on solid state phase transformations, eds. HI Aaronson, DE Laughlin, RF Sekerka, CM Wayman, Met. Soc. of AIME, Warrendale, PA, 813-817.

Zaluzec NJ (1978) "Optimizing conditions for X-ray microchemical analysis in analytical electron microscopy", proceedings of 9th. Intl. Conf. on electron microscopy, ed. JM Sturgess, Microscopical Society of Canada (Toronto) I:548-549.

Zaluzec NJ (1985) "K-shell X-ray cross sections for application to analytical electron microscopy", presented at conference on electron-specimen interactions, Cambridge, 1983, J. Microsc., in press.

Ziebold TO (1967) "Precision and sensitivity in electron microprobe analysis", Anal. Chem. 39, 858-861.

Discussion with Reviewers

A.D. Romig Jr.: I find your use of units of monolayer confusing. Does 0.002 monolayer mean 2 of every 1000 atoms in a monolayer? There has been some nice work done comparing the detection of grain boundary segregation in the AEM to Auger techniques. Have you ever compared FEG-AEM data to Auger data? How did the detectability limits of the techniques compare?

Author: The use of units of a monolayer is as described in the question. In some unpublished work, we have attempted to compare Auger and AEM data on segregation of P at grain boundaries in Ni; we found, however, that the segregation of the P to the free surface was far in excess of that at the grain boundary, and we were unable to reach any conclusions about the analytical techniques.

D.B. Williams: Please explain how figure 2 shows spatial resolution which is not inconsistent with the data of table 2. Why is there no detectable Cr-depletion in the α (ferrite) phase in figure 2?

Author: If we attempt to measure the probe size by taking the distance between the 5% and 95% levels in the chromium profile across the ferrite/cementite boundary (where we know, from the thermodynamics of the partitioning, that the chromium concentration has an abrupt step) we find a figure of 3nm on the left side of the plot of figure 2, and 5nm on the right side. If, on the other hand, we consider the width at half-maximum of the chromium peak just inside the cementite on the left side, we can estimate this to be about 2.5nm. Remembering that the atom probe data showed this peak to be about 2nm wide, it is clear that the STEM analysis is not causing very significant broadening - certainly not by 3 or 5nm. These results are not consistent if the probe has a Gaussian form, and indicate the presence of wide skirts around a sharp central spike, exactly as predicted by Kenway and Cliff (1984) for spherically aberrated probes. The discussion in the paper ignores the presence of the skirts; it is therefore suggested that the small amount of broadening of the chromium peaks is in agreement with the results of this paper, and that the broader skirts in the ferrite are caused by the aberrations in the probe.

Cr-depletion was measured in the ferrite phase, but figure 2 does not extend far enough to illustrate this.

C.S. Pande: It is true that near the Bragg orientations, beam broadening will be less, but these positions are hardly suitable for X-ray analysis because of orientation effects. Please comment.

A.D. Romig Jr.: I find the effects of crystallography on beam broadening fascinating. Has your group ever tried, or do you plan to try, to use the crystallographic effect on spatial resolution to your advantage?

Author: We are very interested in exploring further the effects of crystallography. It is too early to say if it will ever be practical, but one can imagine cases when it would be preferable (contrary to current practice) to orient the specimen deliberately at a Bragg condition to minimize beam broadening. Of course, one would have to consider other effects of crystallography on quantitative analysis. We are planning more experiments to study this.

A.D. Romig Jr.: Your estimate of detectability limit (0.04% Cr in Fe) seems overly optimistic. For example, the estimates of Romig and Goldstein (1979), or Statham (1982) seem more in line with experimental observations. Please comment on older alternative estimates of detectability limit.

D.B. Williams: Other treatments of minimum detectability (Romig and Goldstein, 1979) using Gaussian statistics state that a peak is only detectable if it is $> 3(2N_{eb})^{\frac{1}{2}}$, while your treatment using Poisson statistics predicts $2N_{eb}^{\frac{1}{2}}$ definition of detectability. Can you please explain which answer you consider to be more correct, and why?

Author: The counting of X-rays obeys Poisson statistics; however, for sufficiently large numbers, Poisson statistics and Gaussian statistics converge. The treatment discussed in this paper is valid only if the statistical uncertainty in the background is negligible. Earlier treatments referred to in the questions are correct for the case when the background is fitted to the same number of channels as the peak window. Earlier authors have required a peak to exceed three standard deviations above the background before defining it to be

"detected", while the present paper considers a peak to be detected if it exceeds two standard deviations above the background. The earlier approach has much to recommend it when a wavelength-dispersive detector is in use, as there are more sources of error in that case, but the present author considers it to be unduly restrictive when applied to an energy-dispersive spectrum.

The estimates of detectability limit made in this paper also depend intimately upon the estimates of peak-to-background ratio. These ignore such effects as background arising from the specimen holder or stray electrons, and therefore in practical cases may not have been attained. It is the purpose of the paper, however, to examine the potentials of analytical microscopy in ideal cases, so the use of these values is appropriate.

A.D. Romig Jr.: Reed (1982) has developed a more sophisticated single scattering model. The Reed expression appears to agree with Monte Carlo calculations of beam scattering even in strongly scattering targets - e.g., it applies into the regime where the Goldstein model breaks down. Have you considered using the Reed expression in your studies?

Author: The Reed data could appropriately be used in these calculations. While its use may change the detail of these predictions, the order of magnitude of the results will be preserved. For the time being, it seems unlikely that it will be possible to verify these predictions experimentally with sufficient accuracy to detect the difference.

Additional References

Reed SJB (1982) "The single scattering model and spatial resolution in X-ray analysis of thin foils", Ultramicroscopy 7, 405-410.

Romig AD, Goldstein JI (1979) "Detectability limit and spatial resolution in STEM X-ray analysis: application to Fe-Ni alloys" in "Microbeam Analysis 1979", ed. DE Newbury, San Francisco Press, 124-128.

Statham PJ (1982) "Confidence in microanalysis: lies, damned lies, or statistics?" in "Microbeam Analysis 1982", ed. KFJ Heinrich, San Francisco Press, 1-7.